

Correspondent: J. Walker  
Experimental Facilities  
National Accelerator Lab  
Batavia, Ill.

FTS/Commercial: 312-231-6600 Ext. 453

PRODUCTION OF W's AND STUDY OF DEEP INELASTIC  
REACTIONS BY VERY HIGH ENERGY NEUTRINOS

Y. Cho, L. Hyman, T. Romanowski  
Argonne National Laboratory

O. Fackler, D. Frisch  
Mass. Inst. of Technology

M. Atac, D. Carey, T. Collins, Y. Kang, Q. Kerns, F. Nezrick  
A. Roberts, J. Sauer, R. Shafer, R. Stefanski, D. Theriot, T. Toohig, J. Walker  
National Accelerator Laboratory

J. Keren, S. Meyer, D. Miller  
Northwestern University

W. Cleland, E. Engels  
U. of Pittsburgh

June 10, 1970

PRODUCTION OF W's AND STUDY OF DEEP INELASTIC  
REACTIONS BY VERY HIGH ENERGY NEUTRINOS

ABSTRACT: A spark chamber and scintillation counter experiment using very high energy neutrinos is proposed using a total of  $2 \cdot 10^{18}$  protons at 500 GeV in Area #1 at NAL. The purposes are simultaneously 1) to search for  $\nu + Z \rightarrow Z + \mu^- + W^+$ ;  $W^+ \rightarrow \mu^+ \nu$ ,  $e^+ \nu$ , and various hadron decay modes, 2) to analyze  $\nu + A \rightarrow \mu^- + \Gamma$  ( $\Gamma$  = hadronic products) for large energy and momentum transfers and 3) to search with an unrestricted trigger and good analyzing power for low cross section or exotic reactions in this new energy region.

Names of Ph.D. Experimenters (by institutions; local leader underlined):

Argonne National Laboratory: Y. Cho, L. Hyman, T. Romanowski  
(also Ohio State U.)

Mass. Inst. of Technology: O. Fackler, D. Frisch

National Accelerator Lab: M. Atac, D. Carey, T. Collins,  
Y. Kang, Q. Kerns, F. Neznick,  
A. Roberts, J. Sauer, R. Shafer  
R. Stefanski, D. Theriot,  
T. Toohig, J. Walker

Northwestern U: J. Keren, S. Meyer, D. Miller

U. of Pittsburgh: W. Cleland, E. Engels

Date: June 10, 1970

Correspondent: J. Walker, NAL

INDEX

	<u>Page</u>
I. Cover Page	1
II. Physics Justification.	3
	Figs. 1-3
II-1 <u>W-Search</u>	4
a. Theoretical Background	4
b. Detailed Purpose	5
c. Previous Results	6
d. Competing Experiments	6
	Figs. 4-10
II-2 <u>Deep Inelastic Neutrino Scattering</u>	7
a. Theoretical Background	7
b. Detailed Purpose	9
c. Previous Results	11
d. Competing Experiments	11
	Figs. 11-16
II-3 <u>Low-Cross Section or Exotic Reactions</u>	12
i. 4-Fermion Interactions	12
ii. Lepton Non-Conservation	12
iii. Neutral Currents	13
iv. e- $\mu$ Universality	13
v. Quark and Monopole Search	13
III. Apparatus, Manpower and Cost	14
III-1. Neutrino Beam	14
III-2. Interaction and Detection Apparatus	15
III-3. Data Format and Analysis	16
III-4. Listing of Equipment Cost and Manpower	16
III-5. Time Plan for the Experiment	17

## II. Physics Justification and Experimental Arrangement

We propose an experiment in Beam #1 at NAL with these simultaneous objectives:

- 1) Search for production of the W-meson of weak interactions. A final state  $\mu$ -meson would be observed in association with some of the decay products of the W, namely,  $\mu\nu$ ,  $e\nu$  and some hadronic decay modes.
- 2) A comprehensive study of the deep inelastic scattering of the  $\nu_\mu$  and  $\bar{\nu}_\mu$ . This will be done with a primary emphasis on the large range of energy and momentum transfers that can be observed using a complex nucleus as a target. Coherent nuclear effects will be small.
- 3) Search for low cross-section and new reactions.

These objectives will be taken up in order now with the detection of each reaction given in outline. Figure 1 shows a sketch of the apparatus, and Fig. 2 schematizes the functions of its parts.

Figure 3 shows the expected incident neutrino spectra based on the present design of Area 1 at NAL. Note that for convenience we will usually write equations only for  $\nu_\mu$ , treating  $\bar{\nu}_\mu$ ,  $\nu_e$  and  $\bar{\nu}_e$  as contaminants except where a special effort is made to study their effects (II-2-b and II-3).

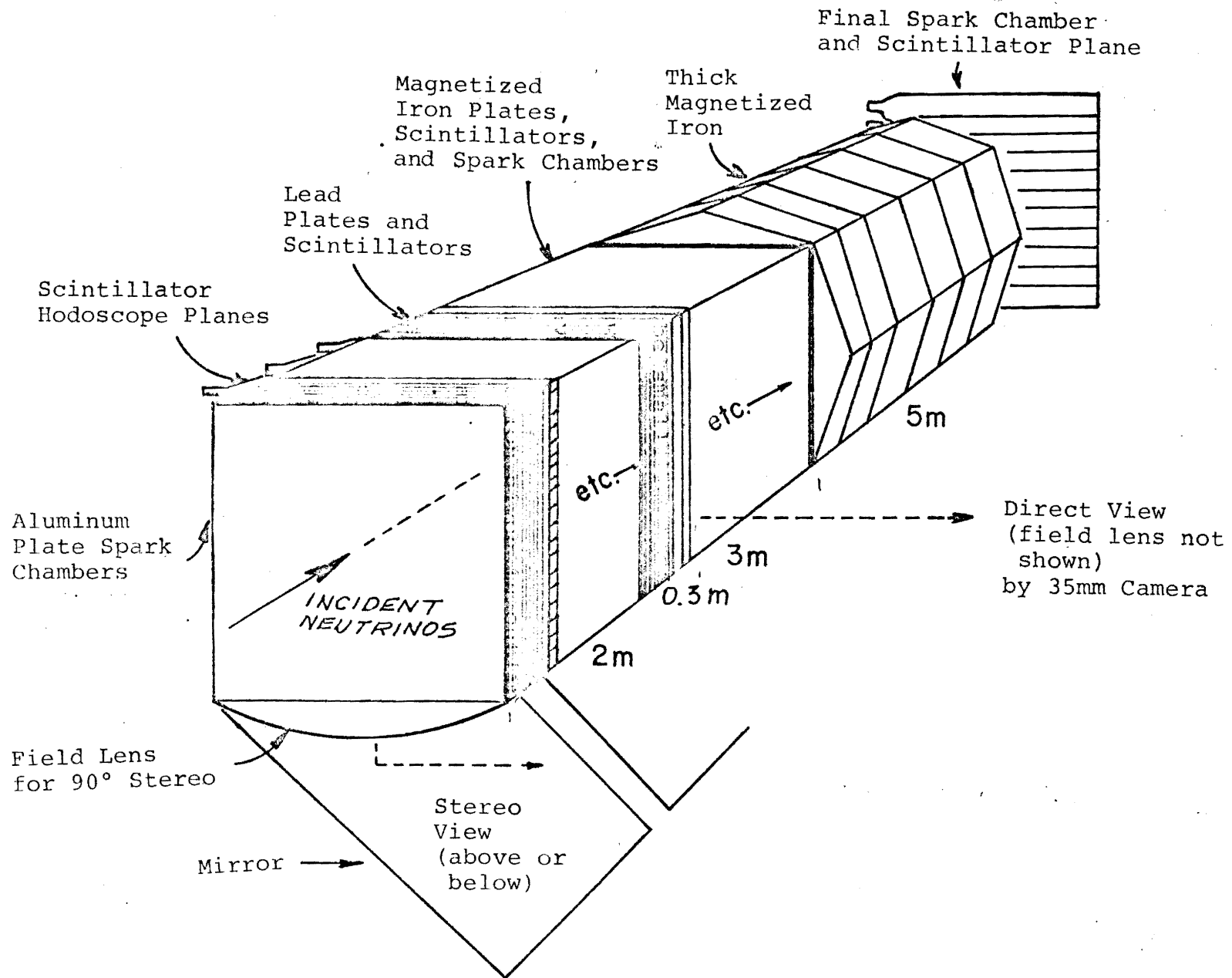
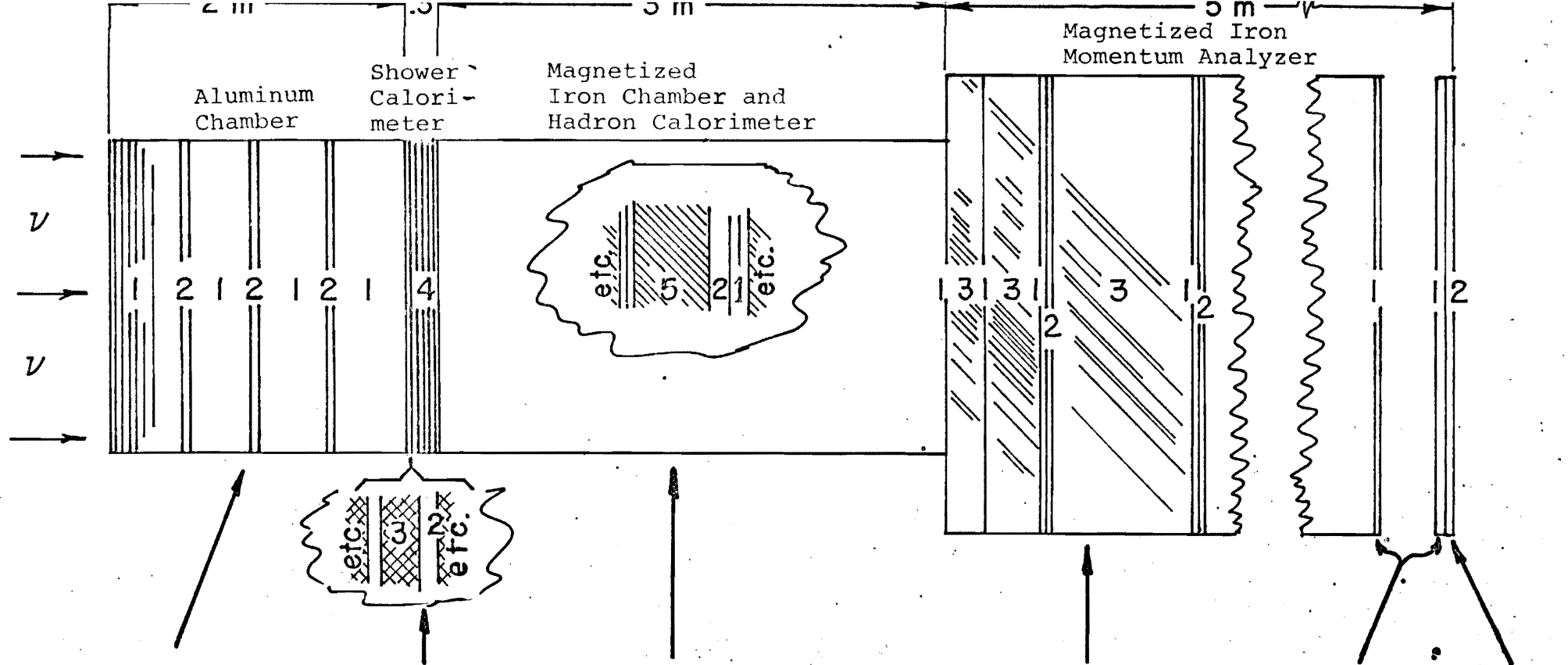


Fig. 1



Components: 1/2" plate Al spark chamber (1), with plane of scin. counters (2) every half meter. Array totals 150 gaps; 11 radiation lengths; 10 tons.

Purposes: Spark chambers give electron, gamma and hadron identification and angle measurements. Scintillators are part of hodoscope trigger throughout apparatus.

1/2 Pb (3) Sandwich with scins (2); 12 layers; 30 radiation lengths; 7 tons.

Electron energy measurement ( $\pm 10\%$ ) by scintillators. Electronic showers removed. Part of hadron showers in Al measured.

2" Fe (5) toroidally magnetized iron sandwich with scins. (2) and spark chambers (1). Totals 30 layers; 1200 gm/cm<sup>2</sup>;

Angle; sign and range of muons measured by spark-chambers for ( $.5 \lesssim E_{\mu} \lesssim 2$  GeV.) Hadron energy ( $\pm 10\%$ ), measured by scintillators ("Hadrometer").

Toroidally magnetized iron (3) with spark chambers (1) and scins. (2). Six sections of iron increasing from 1' to 4'. Totals 300 tons.

Bending magnet gives momentum of higher energy muons ( $> 10$  GeV) to  $\pm 10\%$ . Spark chambers between sections of magnet give range and sign for  $2 \lesssim E_{\mu} \lesssim 10$  GeV.

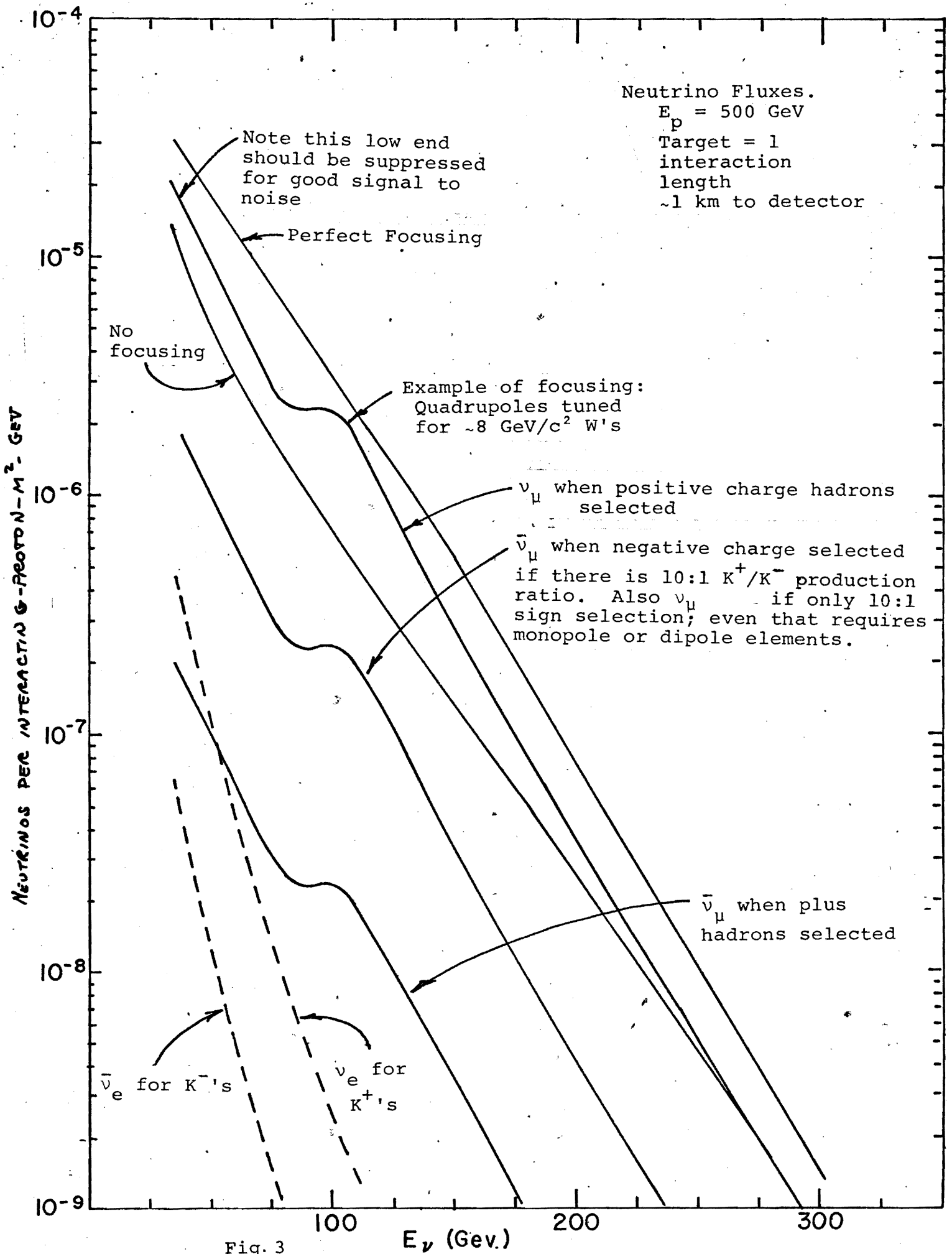
Spark chamber separated by 2'.

Angle of muons emerging.

Last plane of scins

Final hodoscope elements.

Figure 2



II-1 W-Search

$$\nu + Z \rightarrow W^+ + \mu^- + Z \quad \left( \begin{array}{l} \text{coherent} \\ \text{incoherent} \end{array} \right) \quad (\text{Eq. 1})$$

followed by

$$W^+ \rightarrow \begin{array}{l} \mu^+ + \nu \\ e^+ + \nu \end{array}$$

hadrons (e.g.,  $\pi^+\pi^0$ ,  $K^+\bar{K}^0$ ,  $p\bar{\Lambda}^0$ )

II-1-a Theoretical Background

The simplest expectation for the (so far pointlike) weak interactions is that at high enough energies real charged intermediate ("W") mesons can be produced as in Equation 1 and Fig. 4, decaying into leptons ( $\mu\nu$ ,  $e\nu$ ) or hadrons ( $\pi^+\pi^0$ ;  $p\bar{\Lambda}^0$ , etc.). The branching ratios are not firmly predictable, except that  $\mu\nu$  and  $e\nu$  should be almost equal. Observation of large cross sections which were equal for the two leptonic modes would give strong evidence for either W-production or for some other mechanism for an anomalously large 4-Fermion interaction.

The experimental setup we propose has good acceptance for different types of events, so that we are not depending, in this first search, on detailed predictions for W's of e.g., the lepton versus hadron decay branching ratio or the production and decay angular distributions.

Total cross-sections per proton for production of W's of various masses in an iron target are given as a function of neutrino energy in Fig. 5. The differential cross-sections that been calculated by Brown at BNL and Smith at SUNY and Hobbs at MIT. The energy distributions of the  $\mu$ 's are shown in



Fig. 6, and their angular distributions in Fig. 7. The W's are produced almost dead forward, and with almost the full neutrino energy, so that those  $\mu^+$ 's (about half the total) with  $E_\mu > E_\nu/2$  come off with an angle  $\lesssim \frac{M_W}{E_\nu}$

#### II-1-b Detailed Purpose

The detection of W-events is schematized in Fig. 10. A search for charged W mesons over the mass range  $M_W \lesssim 12 \text{ GeV}/c^2$  will be made using  $\nu_\mu, \bar{\nu}_\mu$  and, much less sensitively,  $\nu_e$  and  $\bar{\nu}_e$ . Targets of iron and aluminum will be used. Based on  $\frac{W \rightarrow \mu\nu}{W \rightarrow \text{everything}} = \frac{1}{3}$ , the neutrino fluxes given by Fig. 3, the detector parameters given in Fig. 2, and on acceptance of only those events with  $E_{\mu^-} > 1 \text{ GeV}$ , the expected numbers of W's for different W masses are given in Fig. 8. Figure 9 indicates a measure of the signal to noise.

Thus, about 20  $\mu$ -decay W's with a mass of  $12 \text{ GeV}/c^2$  should be detected with this equipment in a 1000-hour run. ( $12 \text{ GeV}/c^2$  W's are made mostly by neutrinos with  $E_\nu$ 's of  $150 \pm 50 \text{ GeV}$ ). In the high mass region, where few events are expected, the event rate decreases by a factor of about three for every  $1 \text{ GeV}/c^2$  increase in W mass, so a multiplication by three of beam intensity or detector mass is necessary to extend the mass range by  $1 \text{ GeV}/c^2$ . The spectrum we use may easily be low or high by a factor of 10 in the 150 GeV region, so our mass limit should read  $12 \pm 2 \text{ GeV}$ . Note that there is appreciable coherent production only in the low  $M_W$  region, where the high flux gives very high rates anyhow, so choosing iron and

aluminum vs. e.g., lead as the main targets gives little loss, but considerable technical simplification.

The triggers and signatures are given on Fig. 10. The main expected backgrounds against which the W-signatures must be recognized are also tabulated in Fig.10, and are estimated to be less than 10% of the signal. A brief discussion of the flux measurement problem will be given in Section II-2-b.

#### II-1-c Previous Results

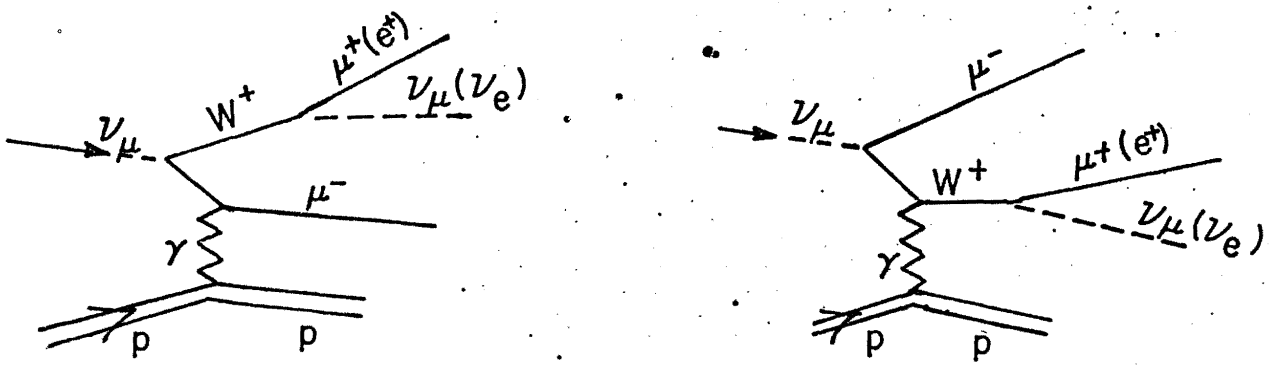
The only fairly sure result of previous experiments is that  $M_W \gtrsim 2 \text{ GeV}/c^2$ .

#### II-1-d Competing Experiments

All competing experiments are only in the planning stage. They are i)  $e^+ + e^-$  colliding beam experiments at CEA, DESY, and possibly Novosibirsk; ii) bubble chamber experiments with neutrinos at Serpukhov and NAL; iii) other spark chamber experiments now being proposed with neutrinos at NAL and Serpukhov. In addition, proton or muon beams may be used at NAL to search for single  $\mu$ 's with high transverse momentum.

With respect to i), the mass range searched in colliding beams will extend up to only about  $3 \text{ GeV}/c^2$ .

With respect to ii), the main differences between a 15' hydrogen BC experiment and our proposal are 1) the tonnage of useful target; less than 1 ton of  $H_2$  versus 50 tons of iron and 5 tons of thin aluminum. In addition, at small  $M_W$ , the coherent production from iron gives a further large factor in its favor, and 2) sensitivity to other decay modes: a 15'  $H_2$  B.C. would give only marginal identification of high energy electrons.



Spins: Initial  
 $S_{z_\nu} = -1/2$

Final  
 $S_{z_W} = -1$        $S_{z_\mu} = +1/2$

Decay distribution of charged lepton:  $\frac{dN_{l^+}}{d\Omega} \propto (1 - \cos\theta_{l^+})^2$

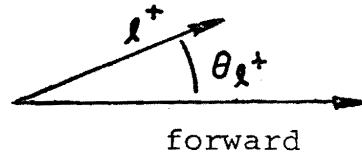


Fig. 4

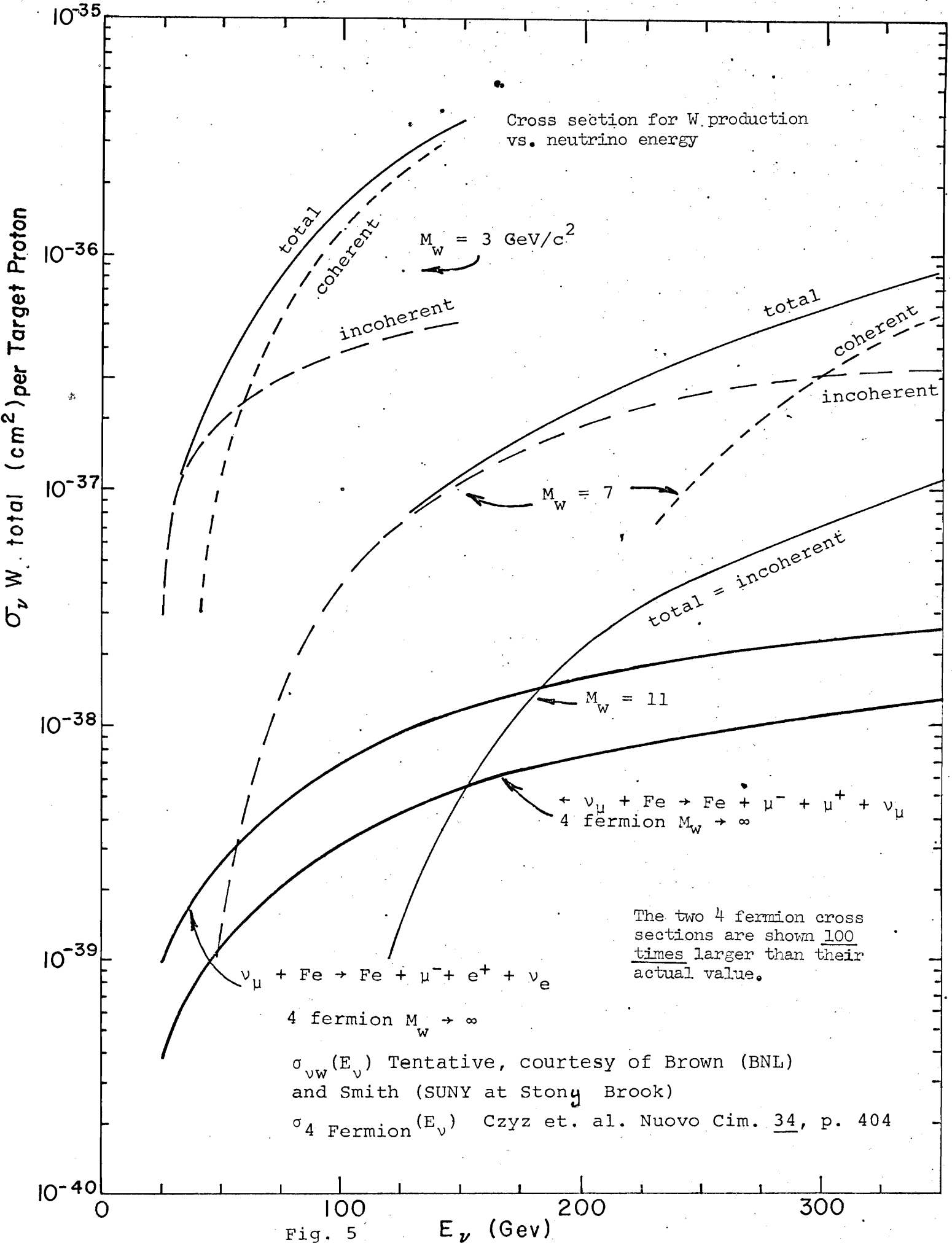


Fig. 5

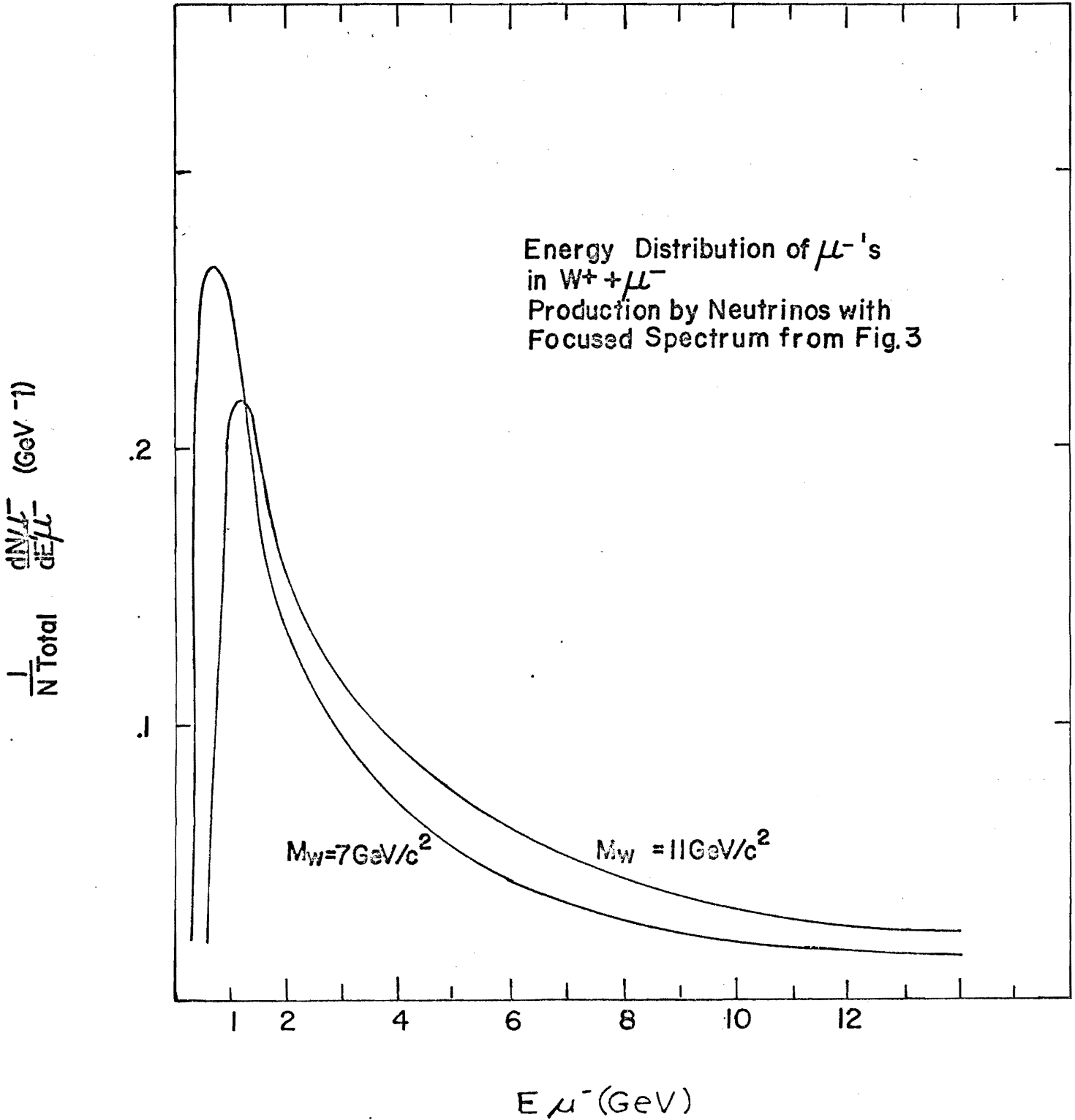
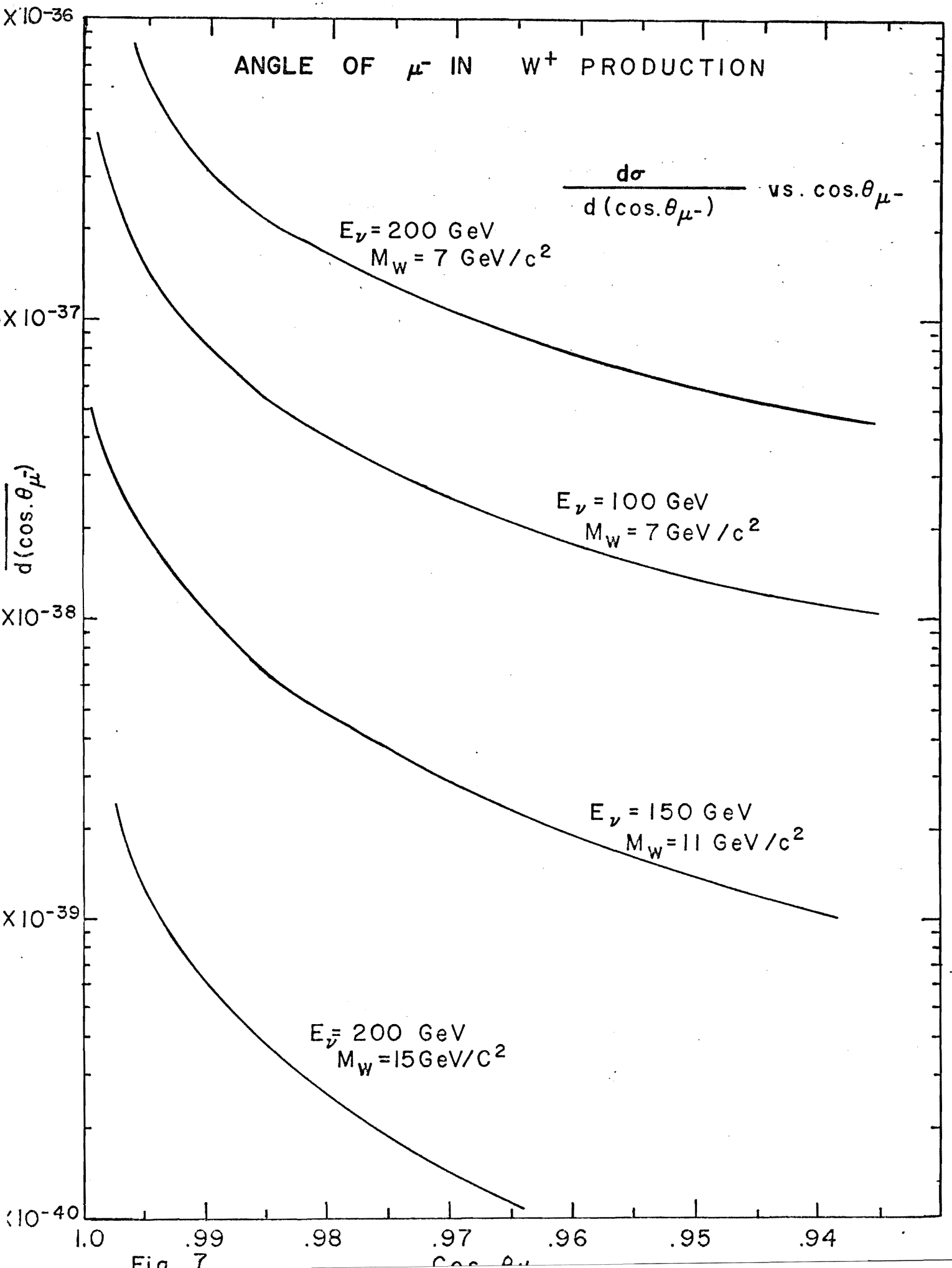


FIG. 6



EVENTS FOR W-MESON PRODUCTION FOR  $\mu^+ \mu^-$  MODE

a)  $2 \times 10^{18}$  INTERACTED PROTONS AT 500 GeV

b) QUADRUPOLE FOCUSED BEAM

c) 50 TON DETECTOR

d)  $(W \rightarrow \mu \nu) / (W \rightarrow \text{all}) = 1/3$

e) 30% DETECTION EFFICIENCY OF  $\mu^+ \mu^-$

NUMBER OF EVENTS

$10^6$   
 $10^5$   
 $10^4$   
 $10^3$   
 $10^2$   
10

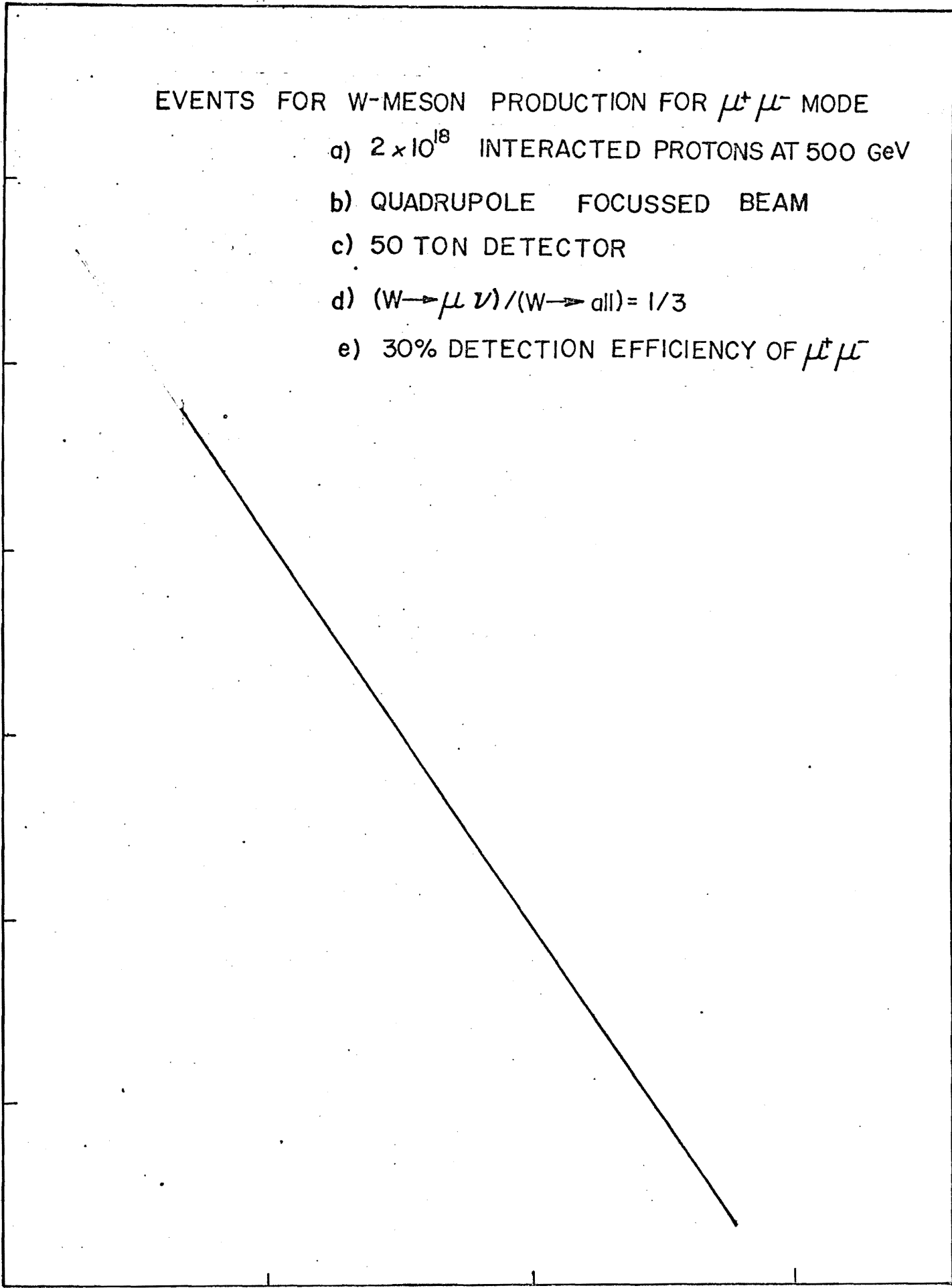
5

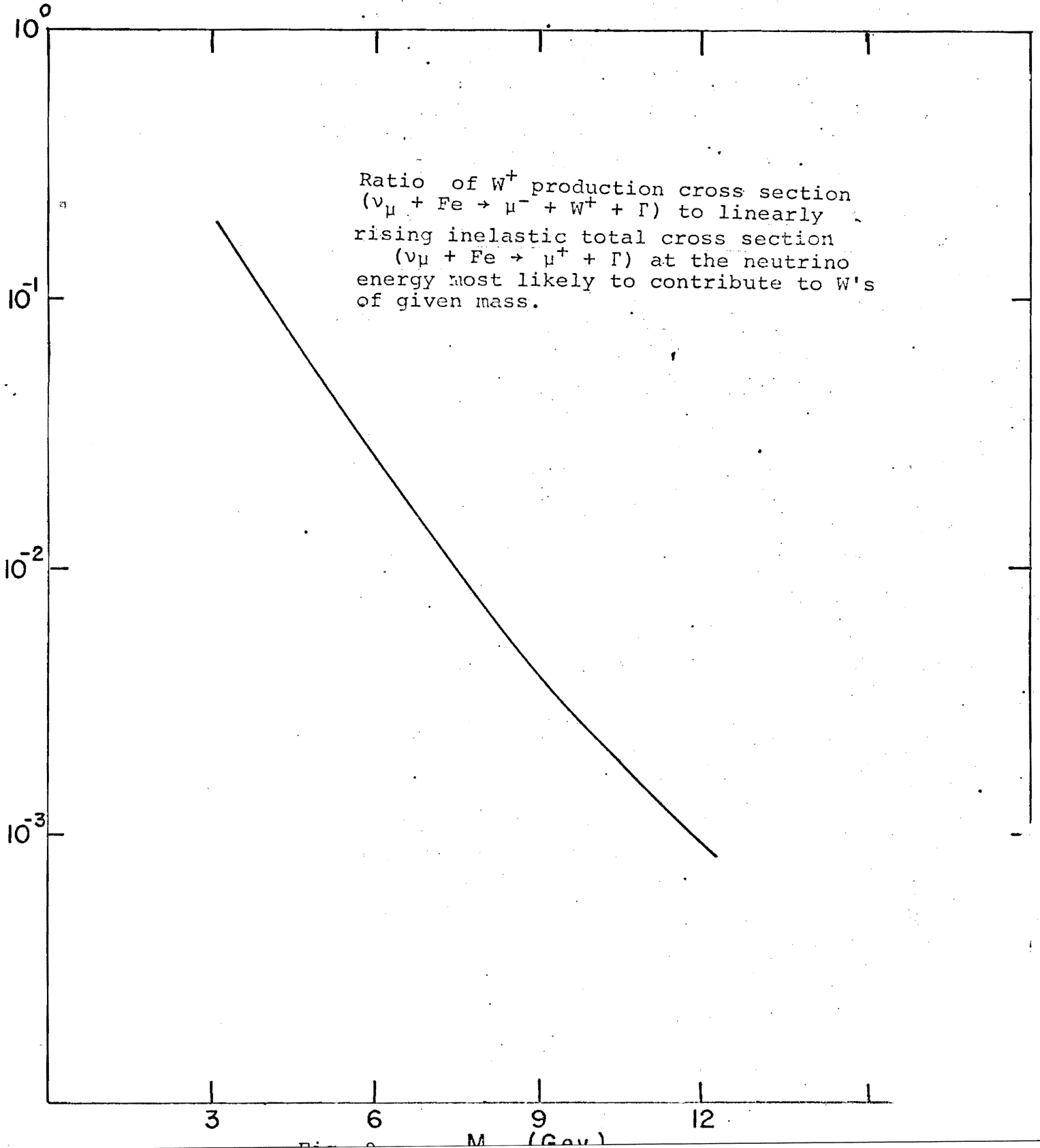
10

15

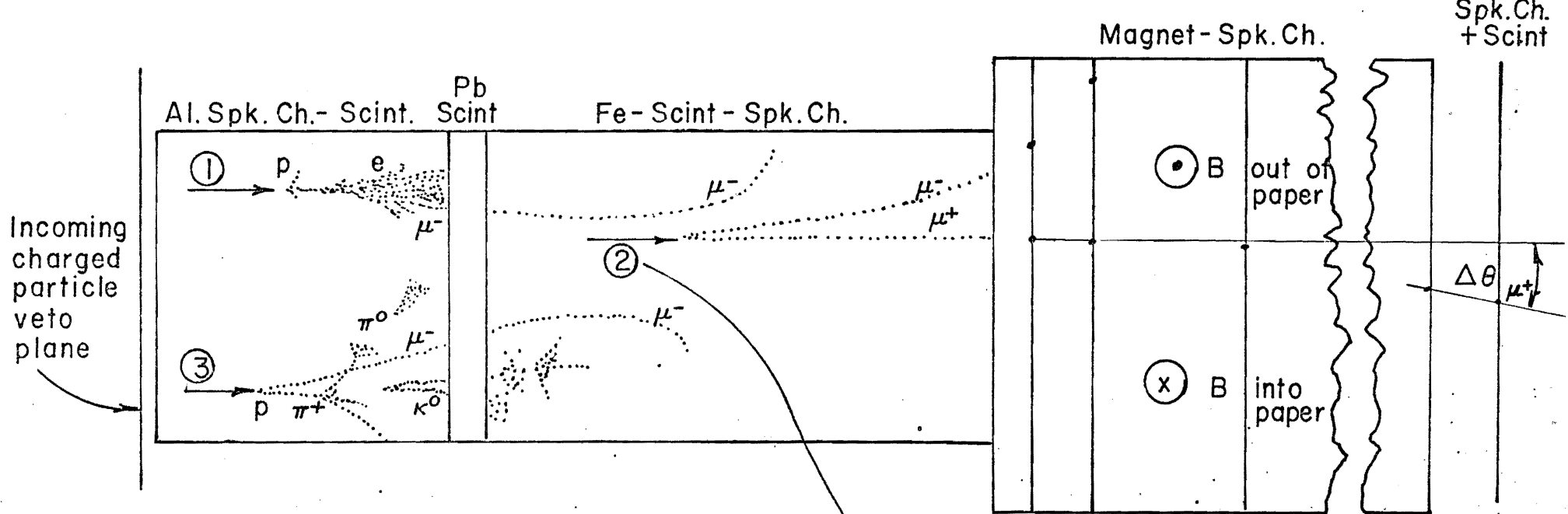
MASS OF W(GeV)

FIG. 8









(Note expect  $\sim 5x$  as many type ② events as others)

Legend on following pages.

SCHMATIC OF W-EVENTS  
FIG. 10

<u>Event</u>	<u>Reaction</u>	<u>Trigger</u>	<u>Signature</u>	<u>Backgrounds</u>
1	$\nu_{\mu} + \text{Al} \rightarrow$ $\Gamma + \mu^{-} + W^{+};$ $W^{+} \rightarrow e^{+} + \nu_{e}$	Big pulse in Pb scintillator and greater than or equal to .3 m track along beam in hodo- scope in Al and Fe.	Not much $\Gamma$ at vertex; greater than or equal to 20 GeV pulse in Pb scintilla- tor sandwich; char- acteristic electron (vs. $\pi^0$ ) shower; $E_{\mu}$ - greater than or equal to 1 GeV	a) $\nu_{\mu} + \text{Al} \rightarrow \text{Al} + \mu^{-} + e^{+} + \nu_{e}$ . (4 Fermion coherent). Identifiable by: no $\Gamma$ ; $\mu^{-}$ usually very forward and high energy. (See Sec. II-3-i).  b) $\nu_{\mu} + \text{Al} \rightarrow \Gamma + \mu^{-}$ ; $\Gamma \rightarrow \pi^0$ giving shower directly or $\pi^{\pm}$ charge exchanging to give shower. Negligible because: very un- likely shower has such high energy and $\mu^{-}$ such low energy; $\Gamma$ would be large and/or shower structure would be different.  c) $\bar{\nu}_{e} + \text{Al} \rightarrow \Gamma + e^{+}$ ; $\Gamma \rightarrow \pi^{-} \rightarrow \mu^{-}$ . Negligible because less than or equal to 1% $\bar{\nu}_{e}$ 's; only approximately 1% of $\pi^{-}$ 's decay before interacting.

<u>Event</u>	<u>Reaction</u>	<u>Trigger</u>	<u>Signature</u>	<u>Backgrounds</u>
2	$\nu_{\mu} + \text{Fe} \rightarrow$ $\Gamma + \mu^{-} + W^{+};$ $W^{+} \rightarrow \mu^{+} + \nu_{\mu}$	Very long track along beam in hodoscopes.	Not much $\Gamma$ at vertex; $E_{\mu^{-}}$ greater than or equal to 1 GeV; $E_{\mu^{+}}$ greater than or equal to 10 GeV; $p_{\perp\mu^{+}}$ greater than 1 GeV/c	<p>a) <math>\nu_{\mu} + \text{Fe} \rightarrow \text{Fe} + \mu^{-} + \mu^{+} + \nu_{\mu}</math> <i>SAME AS 1A</i></p> <p>b) <math>\nu_{\mu} + \text{Fe} \rightarrow \Gamma + \mu^{-}; \Gamma \rightarrow \pi^{+} \rightarrow \mu^{+}</math>. Negligible because: very unlikely <math>E_{\mu^{+}}</math> so high and <math>E_{\mu^{-}}</math> so low; <math>\pi^{+}</math> decays only <math>10^{-4}</math> before interacting.</p> <p>c) <math>\bar{\nu}_{\mu} + \text{Fe} \rightarrow \Gamma + \mu^{+}; \Gamma \rightarrow \pi^{-} \rightarrow \mu^{-}</math>. The ratio of this cross section for that for W production at the <math>E_{\nu}</math> contributing most to W production is shown in Fig. 9, With 30:1 sign selection of the kaons which decay to make the neutrino beam, the <math>\bar{\nu}/\nu</math> ratio should be approximately <math>10^{-2}</math>, and only approximately <math>10^{-2}</math> of the <math>\pi^{-}</math>'s decay before interaction. If the inelastic form factor stays large (Sec. II-2-a), this will give approxi- mately 10% background for <math>M_W = 12</math> <math>\text{GeV}/c^2</math>. Further pulse height and angle discrimination is possible but has not been studied.</p>

<u>Event</u>	<u>Reaction</u>	<u>Trigger</u>	<u>Signature</u>	<u>Backgrounds</u>
3	$\nu_{\mu} + \text{Al} \rightarrow$ $\Gamma + \mu^{-} + W^{+};$ $W^{+} \rightarrow \pi^{+} + K_1^0$ $+ K_2^0$ (an arbitrary example)	Same as 1.	Not much $\Gamma$ at vertex; greater than or equal to 20 GeV pulse in hadrometer; character- istic V's and interactions; $E_{\mu^{-}}$ greater than or equal to 1 GeV.	$\nu_{\mu} + \text{Al} \rightarrow \Gamma + \mu^{-}; \quad \Gamma \rightarrow \pi^{+} + K_1^0 + K_2^0$ Same as 1b.

II-2 Deep Inelastic  $\nu - \mu$  Exchange

$$\nu_{\mu} + A \rightarrow \mu^{-} + \Gamma . \quad (\text{Eq. 2})$$

The kinematics of this reaction are shown in Fig. 11.

II-2-a Theoretical Background

The observation of unexpectedly strong inelastic electron scattering suggests that at least the vector part of the weak interaction can fairly frequently give reactions with very large momentum transfers as in Eq. 2 and Fig. 11.

Assuming the leptonic weak current is local, the differential cross-section may be written as a function of three form factors  $W_1$ ,  $W_2$ , and  $W_3$ . These form factors depend on the two quantities  $q^2$  (the four momentum transfer to  $\Gamma$ ) and  $\nu$  (the energy loss  $E - E'$ ).

It has been found for the corresponding inelastic electromagnetic scattering at SLAC that to a good approximation  $\nu W_2^{\text{e.m.}}$  is a function of the dimensionless variable  $M\nu/|q^2|$  in the region  $|q^2| > 1 \text{ (GeV/c)}^2$  and  $\nu > 1 \text{ GeV}$ . This property has been called scale invariance. Assuming that the vector current is conserved and  $\Delta S = 0$ , it is anticipated that  $W_2$  in the above expression will also exhibit scale invariance and be given by the function  $W_2^{\text{(e.m.)}}$  found at SLAC.

For purposes of illustration we plot  $d^2\sigma/dE'd\cos\theta$  at several angles using a particular model by Drell et.al. wherein  $W_3 = W_2 \frac{2M\nu}{|q^2|}$ ;  $W_1 = \nu W_2 \frac{\nu}{|q^2|}$ . Using the Stanford  $R = 0$  solution

with  $\nu W_2$  a function of  $\frac{2M\nu}{q^2}$  only we obtain for  $E_\nu = 100$  GeV the curves in Fig. 12. We also show for comparison the curve with  $W_3 = W_1 = 0$  at  $\theta = 2.0^\circ$  with  $\nu W_2$  as before. This (dotted) curve can be regarded as a lower limit to the expected cross section, assuming scale invariance continues to hold and also C.V.C. For  $E' = 50$  GeV, for example, the cross section is only very weakly dependent on muon angle. This corresponds to approximately constant  $d\sigma/dq^2$  up to about  $50(\text{GeV}/c)^2$ . In general, the range in both  $q^2$  and  $\nu$  that will be explored in this experiment is roughly one order of magnitude greater than in the corresponding electromagnetic scattering at SLAC.

The remarkable prediction of scale invariance is this very weak dependence of cross section on momentum transfer to the nucleus, with a large number of high energy muons produced at large angles. Observation of these should open up many possibilities for testing models of hadronic structure and dynamics:

1) The total cross-section for Eq. 2 should rise linearly with neutrino energy if  $W_2$  is scale invariant, continuing the CERN observation:  $\sigma_{\nu\mu^-} = 0.6 \times 10^{-38} E_\nu \text{ cm}^2/\text{GeV-nucleon}$ . The effect of a  $10 \text{ GeV}/c^2$   $W$  is shown in Fig. 13.

2) Measurement of the angular distributions for various  $q^2$  and  $\nu$ 's should choose between various models through the ratios  $W_1 : W_2 : W_3$ . In addition, locality of the weak interaction will be tested.

3) Comparison of  $d^2\sigma(\nu)/dq^2 d\nu$  and  $d^2\sigma(\bar{\nu})/dq^2 d\nu$  (averaged

over protons and neutrons in the iron nucleus) over the entire range of  $q^2$  and  $\nu$  will be sensitive to  $W_3$ , which is a highly model-dependent quantity. It can be shown that there can be up to a factor of three difference in the cross sections  $d^2(\nu\text{Fe})/dq^2 d\nu$  and  $d^2(\bar{\nu}\text{Fe})/dq^2 d\nu$ .

4) Comparison of  $\sigma(\nu n)$  with  $\sigma(\nu p)$ .

#### II-2-b Detailed Purpose

The detection of the inelastic scattering reaction is schematized in Fig. 14. It will be studied with incident  $\nu_\mu$  and  $\bar{\nu}_\mu$  over the approximate ranges  $40 < E_\nu < 300$  GeV,  $.5 < q < 10$  GeV/c, and  $.05 < \frac{E_\nu - E_\mu}{E_\nu} < .9$ , and  $20 < E_{\mu^-} < 300$  GeV. The main targets will be 20 effective tons of iron and 5 tons of aluminum. The recoil momenta are so large that there would be little value in using free protons rather than these complex nuclei as targets. Based on scale invariance and on the parameters given in Fig. 14, the expected yield is given in Fig. 15.

A basic difference between this proposal and all previous neutrino experiments is that we propose measuring directly the total hadron energy and the final muon energy. The sum of these two energies will be identified as the incident neutrino energy. Recent results on hadron energy measurements using a scintillator iron sandwich are shown in Fig. 16. It is seen that protons of energy 25 GeV can be measured to  $\pm 2.5$  GeV. We assume that other hadrons give similar results and for simplicity we take  $\frac{\Delta E}{E} = \pm 10\%$ . The magnet for which we have made a

preliminary design will be able to measure muons in the energy range  $10 \leq E_{\mu} \leq 300$  GeV to about  $\pm 10\% \Delta E/E$ . Combining these errors the neutrino energy will be known to roughly  $\pm 10\%$  over the range  $40 \leq E_{\nu} \leq 350$  GeV. Precise knowledge of the incident neutrino flux will require a careful survey of hadron yields, calculation from them of  $\nu$  and  $\mu$  fluxes, and ultimately verification of predicted  $\mu$  fluxes. This is particularly difficult for high neutrino energies, where the more energetic  $\mu$ 's from  $\pi$ 's mask the less energetic  $\mu$ 's from the K's that give the useful high energy  $\nu$ 's. It is likely that the neutrino flux can be determined with confidence to perhaps only  $\pm 20\%$ . But since the flux will almost certainly fall off rapidly with neutrino energy, it will require an absolute accuracy of perhaps 5% or better in the systematics of determination of the average energy of neutrino events through measurement of the  $\mu$  and  $\tau$  reaction products to match even this accuracy. If this is achieved, it will result in absolute neutrino cross sections with errors of the order of  $\pm 30\%$  at all energies.

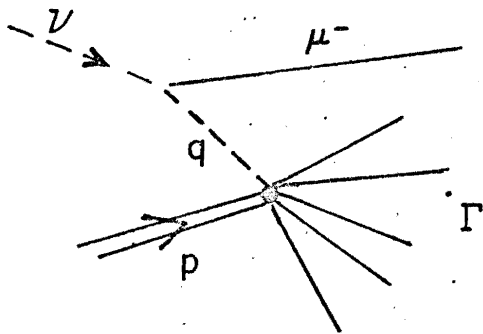
The triggers, signatures and backgrounds are given on Fig. 14.

We are considering the choice between a  $\text{CH}_2 - \text{U}$  comparison and a liquid  $\text{H}_2 - \text{Fe}$  comparison for measuring neutron-proton differences. In any case, the auxiliary target would be upstream of the aluminum chamber and would be only of the order of one interaction length thick.



II-2-c Previous Results: As given in II-2-a above, the CERN results with  $E_\nu < 10$  GeV hint at scale invariance.

II-2-d Competing Experiments: Same as in II-1-d (page 6).



Kinematics:

$E$  is energy of incoming neutrino

$E'$  is energy of outgoing muon

$\Gamma$  represents outgoing hadrons

$q$  is the 4-momentum transfer from leptons to hadrons

$\theta_\Gamma$  is lab angle of 3-vector part of  $q$ , and hence of the core of the hadron jet

$$v \equiv E - E'$$

$$|q^2| \approx EE' \theta_\mu^2$$

$$\theta_\Gamma = \theta_\mu \frac{E'}{\sqrt{q^2 + v^2}}$$

$$M_\Gamma^2 = M^2 + 2Mv - |q^2|, \quad M = \text{NUCLEON MASS}$$

Dynamics:  $\frac{\partial^2 \sigma}{\partial E' \partial \cos \theta} = G^2 E' / 2\pi \left( \frac{E'}{v} \right) \cdot \left[ W_2 \cos^2 \frac{\theta_\mu}{2} + 2W_1 \sin^2 \frac{\theta_\mu}{2} \right. \\ \left. + \frac{E + E'}{M} W_3 \sin^2 \frac{\theta_\mu}{2} \right]$   
 (see p.7)

$G$  is weak interaction constant

$W$ 's are form-factors, functions of  $v$  and  $q^2$ .

FIG. 11

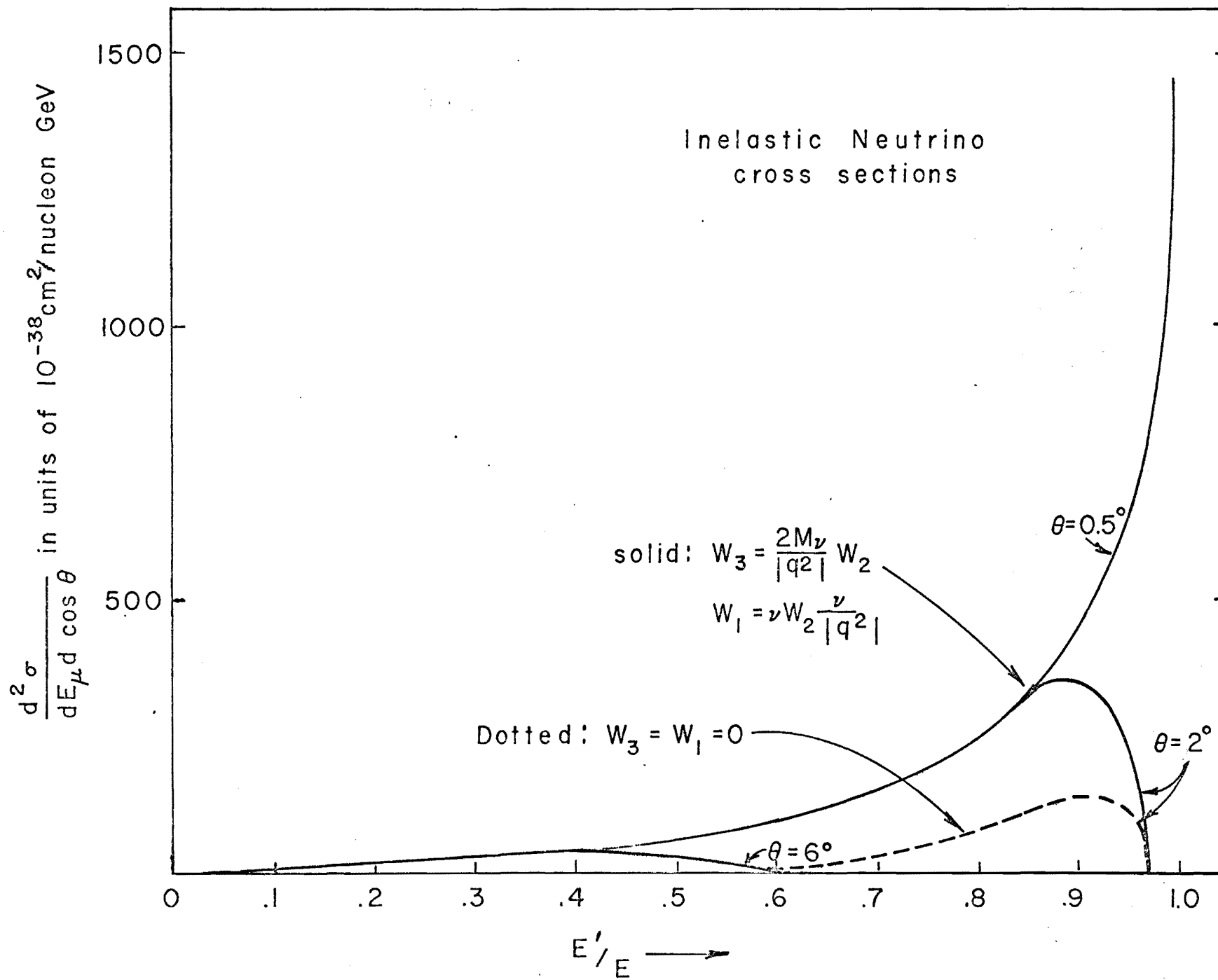


FIG. 12

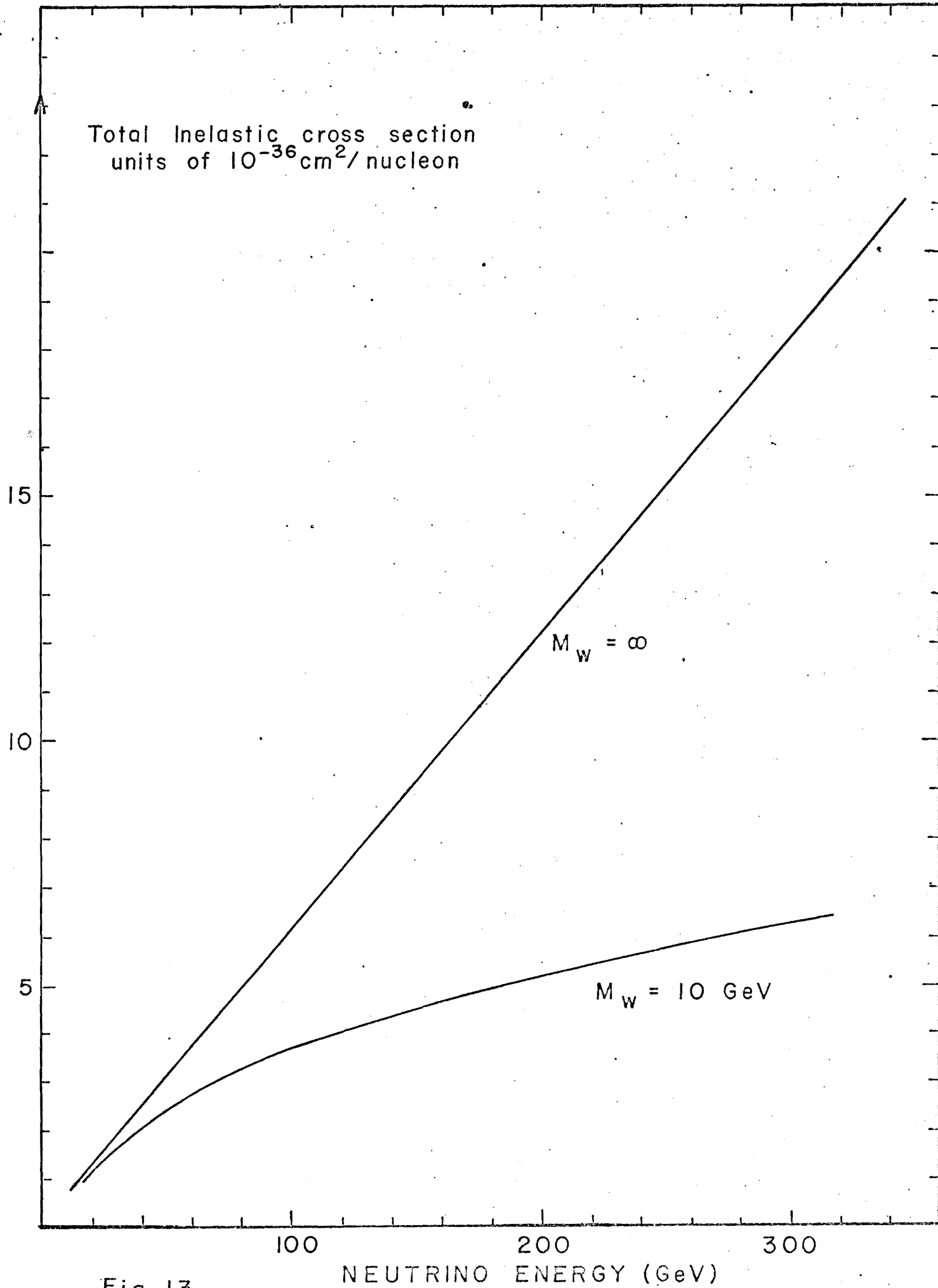
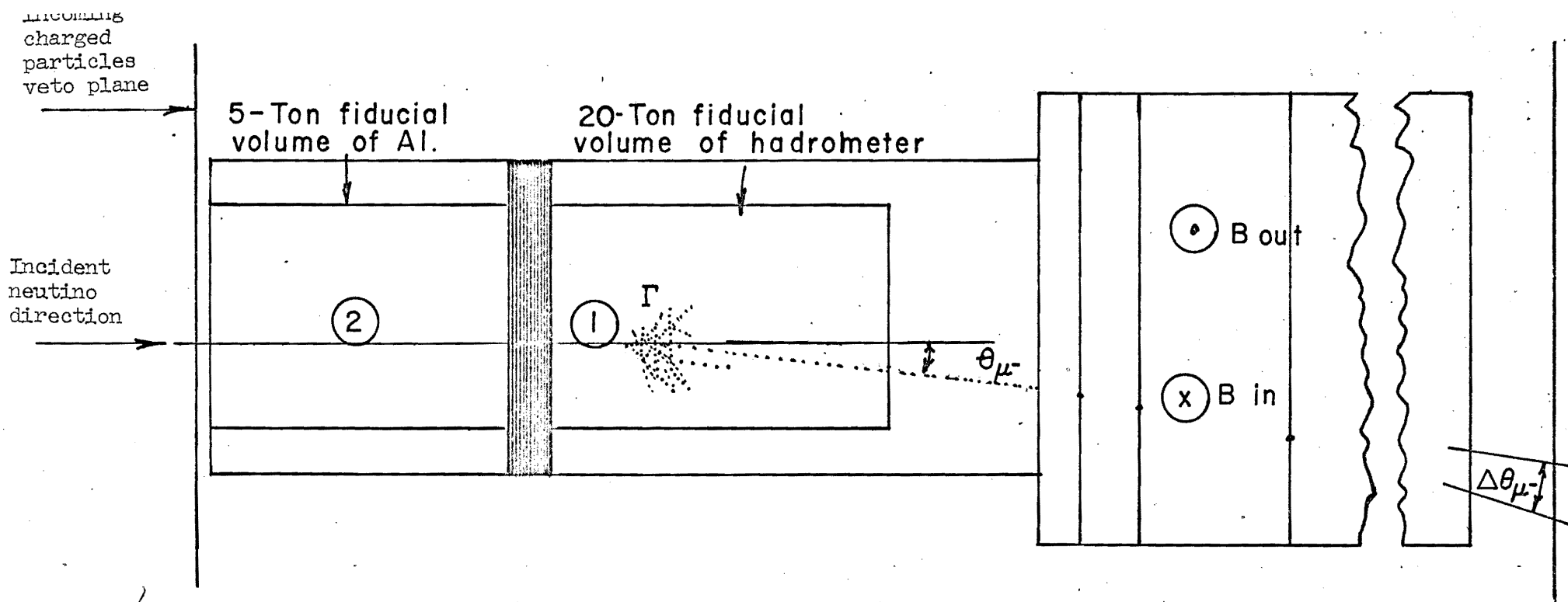


Fig. 13



Event	Reaction	Trigger	Signature	Background
(1)	$\nu + \text{Fe} \rightarrow \mu^- + \Gamma$	Penetrating $\mu^-$ along beam direction	$E_{\mu^-} \rightarrow \sim 20 \text{ GeV}$ ; Big $\Gamma$ pulse and many prongs	$\bar{\nu}_{\mu} + \text{Fe} \rightarrow \Gamma + \mu^+ + W^-$ ; $\mu^- W^- \rightarrow \mu^- + \bar{\nu}_{\mu}$ $E < .5 \text{ GeV}$ in <b>SOME</b> cases, and so indistinguishable from $\pi$ . Negligible if scaling holds but dominant if inelastics down by $10^3$ and a <b>LOW MASS IS PRODUCED</b> (see Fig. 9)
(2)	Same, but in Al	Same as in (1)	Same as in (1). Some of hadron energy in Pb Scint.	<b>SAME AS IN (1)</b>

Fig. 14

Number of Events for  
 $\nu_{\mu} + \text{Fe} \rightarrow \mu^{-} + \Gamma$   
in each interval  $\pm 12\% \frac{\Delta E_{\nu}}{E_{\nu}}$   
for  $2 \times 10^{18}$  interacting  
Protons and a 20 ton fiducial  
volume of detector

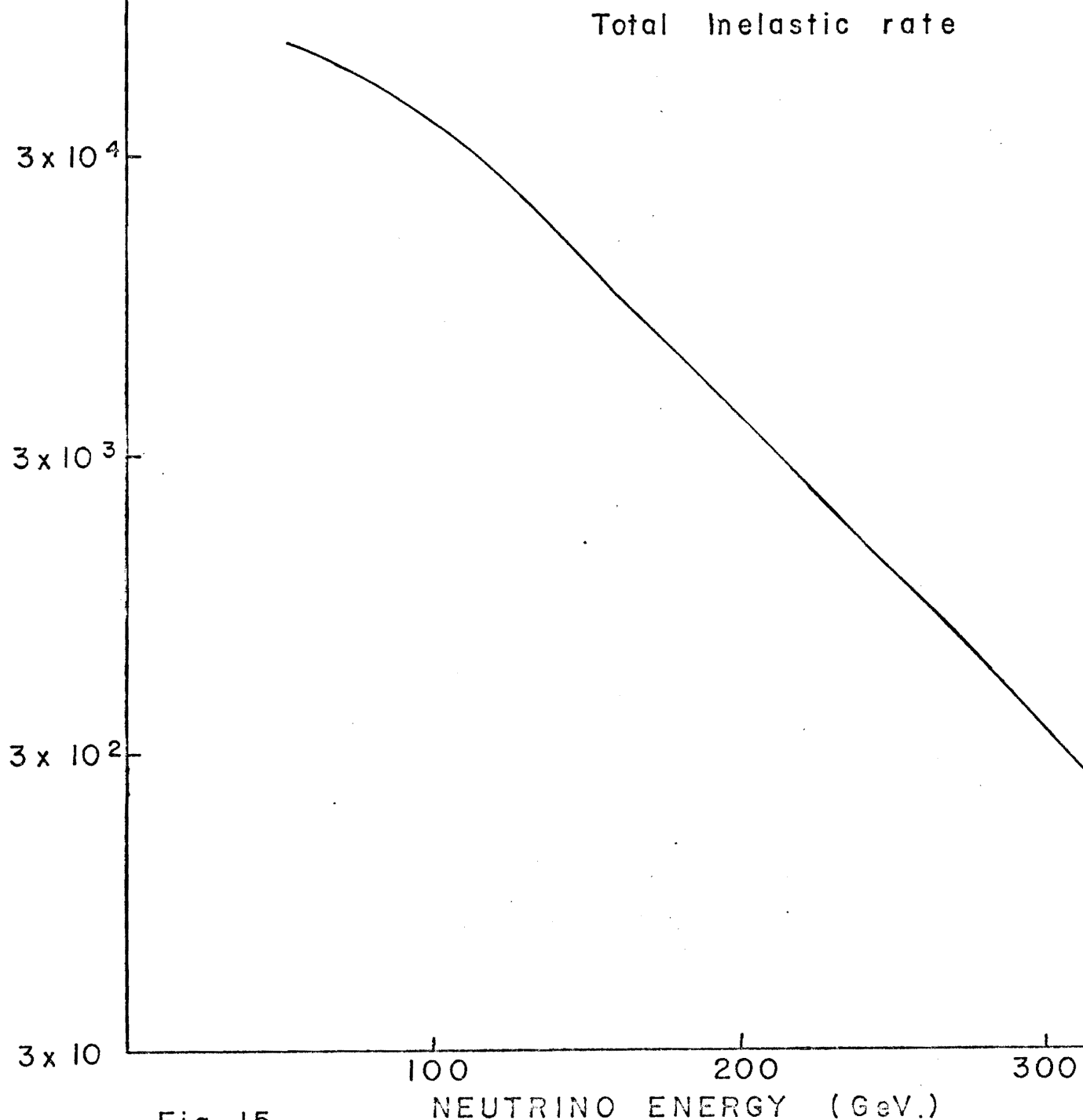
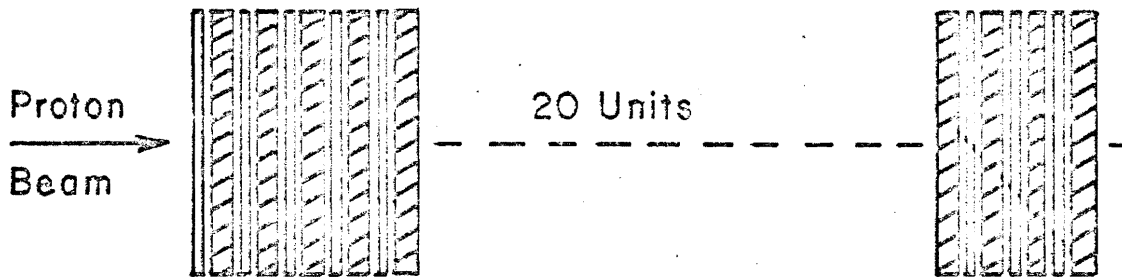
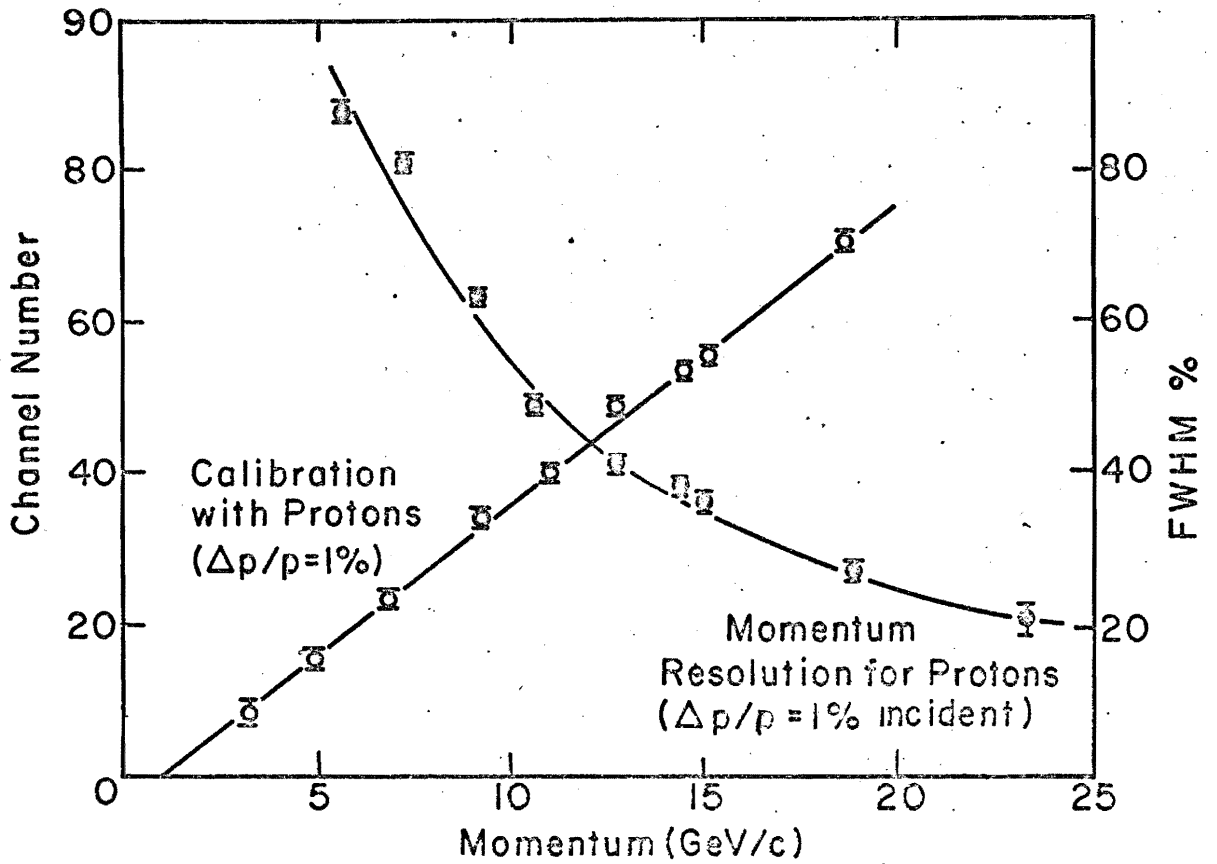



Fig. 15



 =  $20^2 \times 4\text{cm Fe}$

 =  $20^2 \times 2\text{cm Plastic Scintillator}$

Hadron Cascade Total Absorption Counter

Fig. 16

II-3 Low Cross-Section and/or Exotic Reactions:

i. 4-Fermion Interactions: (These are predominantly coherent at these high  $E_\nu$ .)

$$\nu_\mu + Z \rightarrow Z + \mu^- + e^+ + \nu_e \text{ (See Note 1a, Fig. 10)}$$

$$\nu_\mu + Z \rightarrow \mu^- + \mu^+ + \nu_\mu \text{ (See Note 2a, Fig. 10)}$$

The total cross-section for  $\mu^-e^+$  and  $\mu^-\mu^+$  are shown in Fig. 5. The angle and momentum distributions of the charged leptons have been calculated by K. Fujikawa (Ph.D. Thesis, Princeton, June 1970), but with neutrino energies only as high as 40 GeV. While we must await computations at higher  $E_\nu$ , it seems likely that the angular distributions are much narrower for the 4-Fermion interaction than for real W production. We should observe approximately 30 examples of the 4-Fermion  $\mu^-e^+$  from neutrinos with  $50 \leq E_\nu \leq 100$  is from  $100 \leq E_\nu \leq 150$  and 3 from  $150 \leq E_\nu$ . The  $\mu^-\mu^+$  yield should be  $\sim 40\%$  of this. The 4-Fermion reactions should be clearly separated by angle and momentum from real W's.

Observation of the expected cross-sections for the 4-Fermion interactions is complementary to observation of the W, so it is fortunate that the expected yields of these two 4-Fermion reactions are large enough to be measured, and yet small enough not to cause misinterpretation of W-events after kinematic separation.

ii. Lepton Non-Conservation: The ratio of  $\bar{\nu}_\mu + Fe \rightarrow \Gamma + \mu^+$  to  $\nu_\mu + Fe \rightarrow \Gamma + \mu^-$  inelastic cross-sections will be measured. The  $\bar{V}_\nu/V_\nu$  ratio in the beam will be obtained from



the hadron survey. Thus, the  $(\Gamma + \mu^+)/(\Gamma + \mu^-)$  ratio for any given  $q^2$  and  $\nu$  from antineutrino contamination in the neutrino beam is predictable, and should be around  $10^{-2}$ . A disagreement would be an indication of lepton/non-conservation of the  $(\nu \rightarrow \mu^+, \bar{\nu} \rightarrow \mu^-)$  type.

iii. Neutral currents  $\nu_e + e^- \rightarrow \nu_e + e^-$ .

Electron neutrinos in the beam will make electron recoils in the aluminum spark chamber with energies  $\geq 100$  GeV, and with no other reaction product. Since few of the inelastic  $\nu_e + \text{Al} \rightarrow \Gamma + e^-$  events should leave no visible recoil tracks, this exposure should be capable of setting an upper limit in the range on neutral currents at energies  $\geq 100$  GeV.

iv. Electron-Muon Universality.

The reaction  $\nu_e + \text{Al} \rightarrow \Gamma + e^-$  will be compared with  $\nu_\mu + \text{Al} \rightarrow \Gamma + \mu^-$  in the same regions of the  $q^2\nu$  plane. An approximate calculation of the  $\nu_e$  spectrum is shown in Fig. 3.

A comparison to about  $\pm 30\%$  will be possible up to about 50 GeV neutrino energy.

v. Quark and Magnetic Monopole Search:  $\nu_\mu + \text{Fe(Al)} \rightarrow \mu^- \Gamma^+ + \text{quark}$ .

While this is not the equipment of choice for these searches, the many layers of scintillation counters can give pulse height information on the ionization of a penetrating particle.

### III. Apparatus and Cost

#### III-1. Neutrino Beam.

All of the neutrino reaction channels which have been discussed require for their interpretation knowledge of the number of neutrinos in any given energy interval. It is, therefore, of great importance to determine the spectrum and flux of neutrinos. We are willing to take responsibility for hadron surveys appropriate to the needs of this proposal. The primary responsibility for this activity will be taken by the NAL members of our group.

We have discussed earlier the desirability of charge separation of the parent hadrons. Analysis of our experimental goals indicates that we should choose to enhance the high energy end of the neutrino spectrum at the expense of the low energy end. This enables us to keep the trigger open for the rarer high energy events.

We are studying various devices which satisfy the above requirements and we are willing to assume the responsibility to see that sign selection and focusing devices appropriate to this proposal are constructed.

### III.2. Interaction and Detection Apparatus

The interaction and detection apparatus is shown schematically in Fig. 1. The scale of the apparatus is determined mainly by the following considerations:

(a) The diameter of the neutrino beam pipe will be about 35", determining the approximate fiducial diameter of the detection apparatus for hadrometry.

(b) The hadrometer (mean density  $\sim 4$ ) requires about 25 cm around the outer edges to contain the hadron cascade sufficiently well to maintain uniform efficiency and calibration over the inner fiducial region, and about 1 meter at the downstream end of the hadrometer to contain the longitudinal development of hadron cascades produced within the fiducial region. The mass of the fiducial region should be comparable with that of the edges, so that the smallest economical hadrometer meeting these specifications is about what we have designed, 2 m x 2 m x 3 m long. It is close to optimal for these reasons, it matches beam dimensions, and it is a practical size.

(c) The diameter of the long bending magnet must be somewhat larger than that of the hadrometer to accommodate

these high energy muons that go off at angles of the order of  $1/10$  radian; but the cost and inconvenience of subtending very large angles limited our choice to an approximate cylinder 3 meters in diameter, toroidally wound. The length of the iron is set at 5 meters by needing to analyze accurately the bending of 300 GeV muons.

(d) The aluminum (the mean density  $\sim 1.3$ ) spark chamber is 2 meters long, i.e., 11 radiation lengths and 3.5 interaction lengths thick. This enables electrons produced in the aluminum to develop an identifiable shower, and some hadrons produced in the chamber to interact in a characteristic way. Its diameter is set by the rest of the system.

### III-3 Data Format and Analysis

Conventional optical spark chamber techniques will be employed. We have the following approximate available capacity of high accuracy manually operated measuring machines.

M.I.T.	6 machine shifts/day
N.W.	8 machine shifts/day
ANL	3 machine shifts/day
NAL	6 machine shifts/day

This represents an average about 600 effective hours per week of measuring. At a measuring rate of 5 per hour this gives us 10,000 useful events accumulated per month. This is adequate to extract interesting physics rapidly.

### III-4 Listing of Equipment and Cost

The following is a listing of the equipment uniquely

required for this experiment and a rough estimate of the cost including design and labour. These costs are very approximate, since no engineering studies have been made.

<u>Item</u>	<u>Cost</u>
Hadrometer Iron (magnetized) and 5 meter Muon Momentum Analyzing Magnet with frame	\$250 K
Scintillation counters, PM tubes and electronics	\$125 K
Aluminum Spark chamber Modules with Associated Hardware	\$100 K
Spark Chamber Photography (optics, film, etc.)	\$ 50 K
Film Analysis and Computing	\$200 K
Miscellaneous	<u>\$100 K</u>
TOTAL	\$825 K

We have the design experience and the local engineering support at NAL and ANL, to produce the necessary heavy hardware.

#### III-5 Time Scheduling for the Experiment

We propose that this experiment be performed in the following three phases:

1. Hadron Beam Survey

The high hadron (in particular kaon) energies that are relevant for knowing the high energy (300 GeV) neutrino spectrum pose technical difficulties in a conventional beam survey.

However, in pp collisions, due to the fore-aft symmetry of the reaction, low-energy backward kaons can easily be detected and related to fast forward kaons.

We are investigating this scheme for doing a survey of the high-energy yield of kaons and pions at energies up to 500 GeV. This approach was successfully used at the ZGS several years ago, and has been suggested by D. Jovanovich for use at NAL.

The experience at CERN has been that once the pp hadron yields are known, the yields from complex nuclei of low Z can be predicted to  $\pm 20\%$ . This procedure can be checked at kaon energies less than about 150 GeV where K,  $\pi^0$  separation will be technically possible in the early stages. For this check, we propose collaborating with the group using the high energy (150 GeV) survey spectrometer in Area 2, in mid 1972. The data on pion yields will also, as a by-product, be vital engineering information for muon shielding in Area 1. This work will be done primarily by the NAL part of the group.

## 2. Neutrino Beam

In 1972, the Area 1 schedule will begin to allow initial testing of charge separation and neutrino beam production and monitoring. We propose taking responsibility in this work.

### 3. Detection System

The tentative schedule for these chambers and associated systems therefore reads:

- a. Design and construction, Fall 1970 - 12/71.
- b. Preliminary testing, 1/72 - 6/72.
- c. Modifications, if any, 3/72 - 9/72.
- d. Start installation in Area 1, 9/72.
- e. Testing and  $\mu$  and hadron calibration, 1/73.
- f. Ready for experiment, 4/73.

It is worth remarking that not all the running for the experiment needs to be done at 500 GeV; the experiment would be worthwhile at 200 GeV. In particular, much of the testing can be speeded up by running at the higher repetition rates possible at the lower energy.

#### III-6 Equipment and Facilities Required from NAL

1. A suitable building to cover the experimental detection equipment, with the usual utilities, including a 0.25 MW power supply for the muon magnet. A weight of about 500 tons must be supported.
2. Charge separation and focusing magnets for parents of neutrino beam.
3. Support for the hadron beam survey.
4. Proton, muon and neutrino beams monitoring equipment.
5. A small computer for beam flux, etc., monitoring and detection.
6. Electronics, etc., from the NAL Equipment Pool.
7. Use of the hadron and muon beam in Area 1 to calibrate the detection equipment.
8. Film development facilities.